# ANALYSES OF ERRORS ASSOCIATED WITH PHOTOMETRIC DISTANCE IN GONIOPHOTOMETRY

**Jacobs, V.** [1,2]; Blattner, P. [3]; Ohno, Y. [4]; Bergen, A.S.J. [5], Krüger, U. [6];

Hanselaer, P. [2]; Rombauts, P. [1], and Schmidt, F. [6]

[1]Department of Electric Engineering and Energy Technology, Vrije Universiteit Brussel, Belgium;
[2]KU Leuven, ESAT/Light&Lighting Laboratory, Technology Campus Ghent, Belgium;
[3]METAS, Switzerland, [4]NIST, USA; [5]Photometric Solutions International, Australia;
[6]TechnoTeam Bildverarbeitung GmbH, Germany

mailto: valery.ann.jacobs@vub.ac.be

## Abstract

In lighting calculations and simulations, the emission of a light source is conventionally modelled using the far-field intensity, also termed luminous intensity distribution (LID). Previous studies have indicated that the traditional limiting photometric distance, to reach far-field conditions, is not always easy to determine. The "limiting photometric distance", also called the "photometric limiting distance" of a light source is the "shortest distance between the reference plane of a light source and the effective reference plane of a photometer, for a given acceptable error considering the photometric inverse square law" **(ISO/CIE 19476:2014, 2014)**. This distance is dependent on the size of the light source, the luminous intensity distribution (beam angle), the spatial luminance distribution and the predetermined acceptable measurement error. In this paper the problems are analysed in detail for a disk-shaped light source, a linear light strip and a "worst case scenario" using two small (point) sources separated by a certain distance. The limiting photometric distance is investigated using different measures of error - not only for the main illumination direction but also at different angles of emission.

*Keywords*: limiting photometric distance, far-field, near-field, goniophotometry

## 1 Introduction

In far-field conditions, the "luminous intensity distribution" (LID) of a light source can be calculated from the illuminance distribution at a given distance using the "inverse-square-law" which state that illuminance decreases with the square of the distance to the source, and the "cosine law",:

$$I = \frac{E \cdot R^2}{\cos \alpha_\mathrm{r}}, \tag{1}$$

where

- $I$ is the luminous intensity of the source in a given direction;
- $E$ is the measured illuminance by a detector;
- $R$ is the distance between the source and detector;
- $\alpha_\mathrm{r}$ is the polar angle between the local surface normal describing the orientation of the photometer and the direction vector from the detector towards the photometric centre of the source.

The same relationship is used to determine the LID itself. A traditional far-field goniophotometer is equipped with a photometer and from the measured illuminance, the intensity is calculated using the same formula. In practice, the LID is determined at a finite distance and will be termed the "apparent intensity" in this paper, while theoretical calculations of the LID in the limit of infinite distances, result in the true "far-field intensity". The limiting photometric distance can then be defined as that distance where the difference between the apparent intensity and the far-field intensity is below a given threshold, typically 1%.

In literature, the limiting photometric distance is stated to be at least five times the maximum dimension of the luminaire for near-Lambertian sources. This “practical” minimum measurement distance is based on the difference between two determinations of the luminous intensity at different distances along the optical axis of the luminaire; if it is smaller than a predefined threshold, typically 1%, the limiting photometric distance is said to be reached (CIE 070-1987, 1987). Using this criterion, a previous study (Moerman & Holmes, 1981) modelled floodlights analytically and showed that the limiting photometric distance may increase significantly for sources with narrow beam optics.

Nowadays, large luminaires with narrow beam optics are widespread. Examples are surgical luminaires, road lighting and decorative lighting. Narrow beams with a full width at half maximum (FWHM) of only 4° can be attained for LEDs with focusing optics. Existing guidelines today indicate that a minimum measurement distance of 15 times the maximum dimension of the luminaire should be used for non-Lambertian sources (CIE 121-1996, 1996). A new international standard test method for LED luminaires uses a range of minimum test distances based on the beam angle of the luminaire and introduces a “D + S” scenario for luminaires which have large non-luminous spaces within their luminance distribution, where the size of the non-luminous space is added to the overall size in calculating the required test distance (CIE S 025/E:2015, 2015). Recent studies indicate that even more stringent requirements are necessary. (Sun C-C, 2009) calculated a far-field condition for LEDs and LED arrays which showed that far-field conditions are often met at far larger distances than conventional guidelines suggest (Moreno I, 2009). Their conclusions were experimentally validated by the study (Jacobs, et al., 2014) using a 2 LED array and a 5 LED array. Moreover, some studies argue for using a criterion based on a weighted average of the luminous intensity obtained in a number of angular directions. (Moreno I, 2009)

## 2 The limiting photometric distance

Consider an elementary source element $\mathrm{d}A_\mathrm{s}$, on the extended light source $A_\mathrm{s}$, located by a vector $\mathbf{r}_\mathrm{s}$, as in Figure 1(a). The luminance distribution function can be written as

$$L(\mathbf{r}_\mathrm{s}, \alpha_\mathrm{s}, \beta_\mathrm{s}), \tag{2}$$

where

$\alpha_\mathrm{s}$ is the local polar angle between the direction vector towards $P$ and the local surface normal $\hat{\mathbf{n}}_\mathrm{s}$ at $\mathrm{d}A_\mathrm{s}$, and

$\beta_\mathrm{s}$ is the local azimuthal angle with respect to an arbitrary direction.

In far-field conditions, the source can be approximated by a point source, located at the photometric center $C$, as in Figure 1(b). Within the lighting community, the $C-\gamma$ coordinate system is traditionally used as follows: at the photometric center $C$ three mutually perpendicular axes can be defined, which are typically denoted first (or principal or optical) axis, second axis and third axis. The luminaire is oriented in the plane spanned by the second and third axis. If the luminaire is more extended in one direction, as for example rectangular luminaires, the second axis is oriented along the shortest side of the luminaire. Perpendicular to the second and third axis, lies the first axis. The photometric center of the luminaire is the intersection of these axes. Distances can be calculated from this photometric center and angles are specified with respect to the first and second axis. Whenever distances or angles are measured with respect to the photometric center, a bar will be used to indicate this by notation: $\bar{\beta}_\mathrm{s}$ corresponds to the angle of the $C$-plane, and $\bar{\alpha}_\mathrm{s}$ corresponds to $\gamma$.

The apparent intensity of a light source is defined as a function of the luminance distribution in (Jacobs, et al., 2014) by

$$I_\mathrm{app}\left(\bar{R}, \bar{\alpha}_\mathrm{s}, \bar{\beta}_\mathrm{s}\right) = \frac{\bar{R}^2}{\cos\bar{\alpha}_\mathrm{r}} \int_{A_\mathrm{s}} \frac{L(\mathbf{r}_\mathrm{s}, \alpha_\mathrm{s}, \beta_\mathrm{s}) \cos\alpha_\mathrm{s} \cos\alpha_\mathrm{r}}{R^2} \, \mathrm{d}A_\mathrm{s} \tag{3}$$

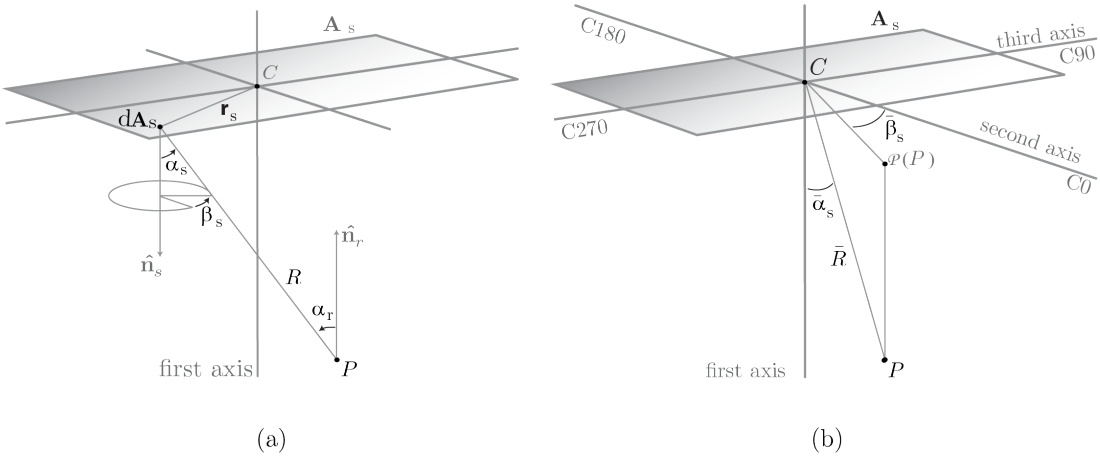


**Figure 1: Coordinates used to determine the apparent luminous intensity of a general light source with an arbitrary luminance distribution. (a) Local coordinates, (b) coordinates with respect to the photometric center $C$ of the light source, where bars are added to the coordinates.**

The far-field intensity $I_{\mathrm{FF}}$ can be written as:

$$I_{\mathrm{FF}}(\bar{\alpha}_{\mathrm{s}},\bar{\beta}_{\mathrm{s}}) = \cos\bar{\alpha}_{\mathrm{s}} \int_{A_{\mathrm{s}}} L(\mathbf{r}_{\mathrm{s}},\bar{\alpha}_{\mathrm{s}},\bar{\beta}_{\mathrm{s}})\, dA_{\mathrm{s}} \tag{4}$$

**Definition.** The angular distribution of the limiting photometric distance can now be defined for each direction $(\bar{\alpha}_{\mathrm{s}},\bar{\beta}_{\mathrm{s}})$ as that distance $\bar{R}$ where the relative error between the apparent intensity $I_{\mathrm{app}}$ and the far-field intensity $I_{\mathrm{FF}}$ is less than a predefined error, for example 1%:

$$\bar{R} \quad \Big| \quad \epsilon(\bar{R},\bar{\alpha}_{\mathrm{s}},\bar{\beta}_{\mathrm{s}}) = 1 - \frac{\mathrm{I}_{\mathrm{app}}(\bar{R},\bar{\alpha}_{\mathrm{s}})}{I_{\mathrm{FF}}(\bar{\alpha}_{\mathrm{s}})} < 1\% \tag{5}$$

## 3 A luminance model for Lambertian sources and narrow beams

For luminaires with focusing optics creating a rotationally symmetric beam, the luminance in each point of the source can be modelled by

$$L(\mathbf{r}_{\mathrm{s}},\alpha_{\mathrm{s}},\beta_{\mathrm{s}}) = L_0(\mathbf{r}_{\mathrm{s}})\cos^n \alpha_{\mathrm{s}}, \tag{6}$$

where

$n$ determines on the full width at half maximum (FWHM or $\alpha_{50}$) commonly used to describe the width of a distribution through

$$\cos^n(\alpha_{50}/2) = 0.5. \tag{7}$$

The higher the value for $n$, the more narrow the beam will be, as in the upper panel of Figure 3.

## 4 Limiting photometric distance of a uniform disk source

The limiting photometric distance of a uniform disk source (see Figure 2) is calculated in (Jacobs, et al., 2014). From Eq. (3), the apparent luminous intensity along the optical axis of a uniform disk source at a point $P$ can be calculated in general.

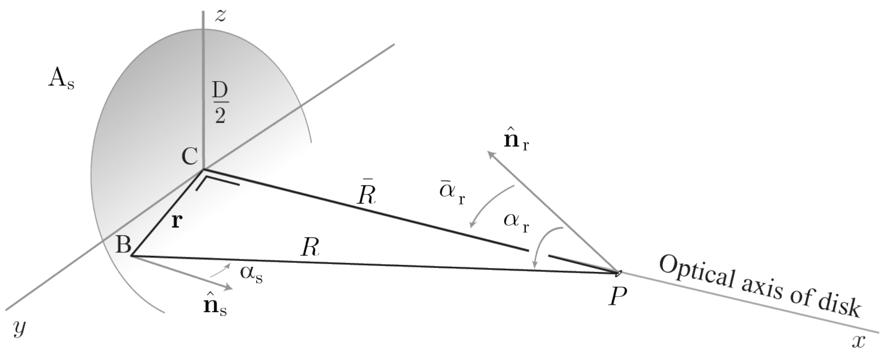


**Figure 2: Coordinates used to determine the apparent luminous intensity of a uniform disk source along its optical axis.**

If $P$ lies on the optical axis, and the surface normal of the surface and receiver are parallel, then $\cos\alpha_r = \cos\alpha_s = \bar{R}/R$, $R^2 = \bar{R}^2 + r^2$ and $\cos\bar{\alpha}_r = 1$. The apparent luminous intensity along the optical axis can be calculated for various beam angles $n$:

$$\mathrm{I}_{\text{app,disk}}\left(\bar{R},0,0\right) = \frac{2\times\pi\, L_0\, \bar{R}^2}{n+2}\left[1-\left(1+\left[\frac{D}{2\bar{R}}\right]^2\right)^{-\frac{1}{2}(n+2)}\right] \tag{8}$$

The far-field luminous intensity along the optical axis can be calculated by,

$$I_{\text{FF}} = \pi\, \mathrm{L}_0 \left(D/2\right)^2. \tag{9}$$

Dividing Eq. (8) by Eq. (9), the ratio between the apparent and far-field intensity can be calculated for various values of $(n)$, as in (5). The relative error $\epsilon$ between the far-field intensity and the apparent intensity can be calculated as a function of the distance to the source along the optical axis

$$\epsilon(\bar{R},0,0) = 1-\frac{\mathrm{I}_{\text{app,disk}}}{I_{\text{FF}}} = 1-8\times\frac{1}{n+2}\left(\frac{\bar{R}}{D}\right)^2\left[1-\left(1+\frac{D^2}{4\times\bar{R}^2}\right)^{-\frac{1}{2}(n+2)}\right]. \tag{10}$$

Confirming earlier studies (Moerman & Holmes, 1981), (Sun C-C, 2009) and (Moreno I, 2009), Eq. (10) allows us to verify that for a Lambertian source ($n=0$) the difference between the apparent intensity and luminous intensity along the optical axis is smaller than 1% from a distance of 5 times the diameter of the disk. This verifies the commonly-accepted principle that the limiting photometric distance for a Lambertian source equals five times the maximum size of the circular luminaire.

For more narrow beams, a larger limiting photometric distance is found. Eq. (8) can be expanded into a power series if $D^2/4\bar{R}^2 << 1$, i.e. at large distance with respect to the dimension of the source.

$$\mathrm{I}_{\text{app,disk}}\left(\bar{R},0,0\right) \cong \pi\, L_0\left(\frac{D}{2}\right)^2\left[1-\frac{n+4}{8}\left[\frac{D}{\bar{R}}\right]^2+\mathrm{O}\left(\left[\left(\frac{D}{2\bar{R}}\right)^2\right]^3\right)\right], \tag{11}$$

where

$O$ defines the sum of all higher order terms in the expansion

Now the relative error can be approximated by dividing Eq. (11) by Eq. (9). An upper bound on the error is then given by:

$$\epsilon(\overline{R},0,0) = \frac{n+4}{8}\left[\frac{D}{\overline{R}}\right]^2. \qquad (12)$$

Using Eq. (12), and $\epsilon = 1\%$, the limiting photometric distance is plotted as a function of the beam width $n$ in the lower panel of Figure 3 and some values are calculated in Table 1. The upper graph of Figure 3 simultaneously displays the relation between the beam width $n$ and the full width half maximum (FWHM) of the beam. Clearly, for narrow beams, the limiting photometric distance is far beyond any current guidelines adopted in the lighting community, for example (CIE S 025/E:2015, 2015).

**Table 1- Typical values for the photometric limiting distance for a circular luminous disk**

| $\epsilon(\overline{R},0,0)$ | | $\overline{R}/D$ | | | | | | |
|---|---|---|---|---|---|---|---|---|
| | | 5 | 10 | 15 | 20 | 30 | 50 | 100 |
| $n$ | 0 | 1,0% | 0,2% | 0,1% | 0,1% | 0,0% | 0,0% | 0,0% |
| | 1 | 1,2% | 0,3% | 0,1% | 0,1% | 0,0% | 0,0% | 0,0% |
| | 5 | 2,2% | 0,6% | 0,2% | 0,1% | 0,1% | 0,0% | 0,0% |
| | 10 | 3,4% | 0,9% | 0,4% | 0,2% | 0,1% | 0,0% | 0,0% |
| | 20 | 5,7% | 1,5% | 0,7% | 0,4% | 0,2% | 0,1% | 0,0% |
| | 40 | 10,2% | 2,7% | 1,2% | 0,7% | 0,3% | 0,1% | 0,0% |
| | 180 | 34,5% | 10,7% | 4,9% | 2,8% | 1,3% | 0,5% | 0,1% |

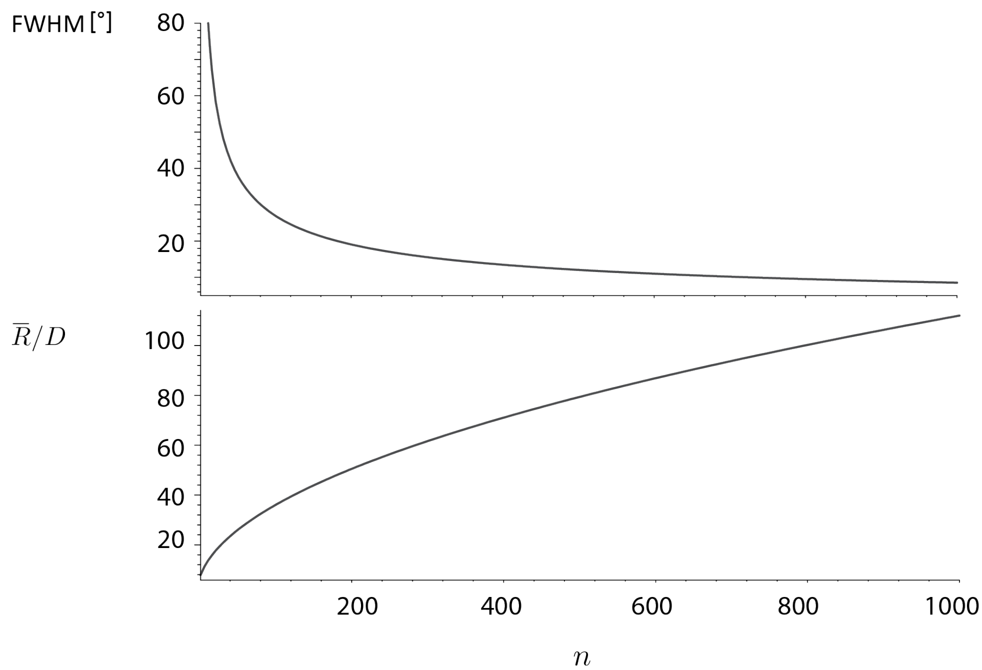

**Figure 3: Circular luminous disk. Upper panel: the FWHM is plotted as a function of $n$ by solving Eq. (7). Lower panel: the limiting photometric distance (expressed with respect to the diameter of the circular disk) to reach an error below 1% is plotted using Eq. (12).**

## 5 Limiting photometric distance for a Lambertian and quasi-1D light strip having a Lambertian distribution

Consider a "linear" light strip of length $D$, tilted by angle $\gamma$. An infinitesimal small detector is located at distance $\bar{R}$ from the photometric center $C$ of the linear luminaire.

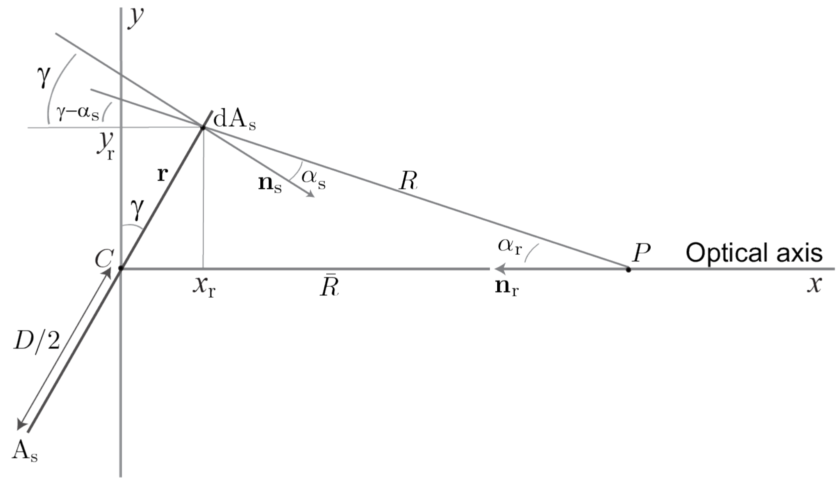


**Figure 4 – A linear luminaire of length D is tilted by an angle $\gamma$.**

Radiation transfer between two (Lambertian like) surfaces (n=0) can be expressed using a configuration factor (or geometrical correction factor), as in (Howell, et al., 2010):

$$F_{1-2} = \int_{A_2} \frac{\cos\alpha_r \cos\alpha_s}{\pi S^2} \mathrm{d}A_s \qquad (13)$$

The different quantities are defined as following:

$$S = \sqrt{(\bar{R} - x_r)^2 + y_r^2} \qquad (14)$$

where

$y_r = r\cos\gamma \qquad x_r = r\sin\gamma$ and

$\cos\alpha_r = \dfrac{\bar{R} - x_r}{R}$ and $\alpha_r = \gamma - \alpha_s$

Eq. (13) can be evaluated numerically, and used to calculate the error of luminous intensity determination if the detector is located too close to the luminaire. The results are shown in Figure 5. The error for different title angles ($\gamma$ = 0°,10°,20°,30°...80°) and ratios of detector-distance-to-luminaire-length are shown. For larger angles, for example 70°, the a ratio of 5 for $\bar{R}/D$ will generate an error of 5,6%, as indicated by the black square in Figure 5.

Figure 5 shows that the error increases dramatically for the off-axis case and this should be taken into account especially for the calculation of partial luminous flux values.

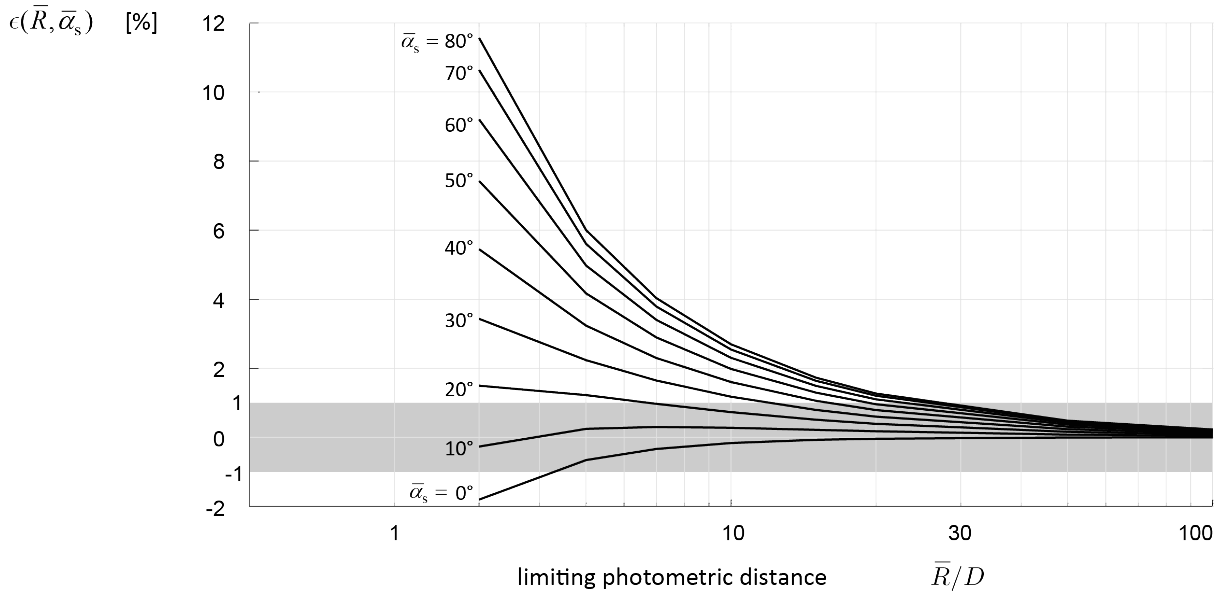


**Figure 5 – The limiting photometric distance is shown for a luminous strip for various angles $\bar{\alpha}_s = 0 \ldots 80°$. The grey band in the middle indicates the region where the error is below 1%. Beyond 30 times the size of the strip, the limiting photometric distance is reached for all angles.**

In order to validate the formula and the matrix-oriented software code, an analytical solution can be found for on-axis illuminance, corresponding to the line where $\bar{\alpha}_s = 0°$ in Figure 5. Without more detailed explanation one will get (Howell, et al., 2010):

$$\epsilon(\bar{R},0,0) = -\frac{1}{6}\left(\frac{D}{\bar{R}}\right)^2 \tag{15}$$

This is the on-axis error of the far-field measurement of a luminaire with length $D$ at a distance $\bar{R}$.

## 6 Limiting photometric distance using a point source approach

The third approach given in this paper is based on a worst case scenario assuming a measurement of a luminaire with two small (point) light-emitting areas separated by a distance $D$. This is a worst case scenario of an extended light source.

The LID of both single light sources is the sum of the two single LIDs. The measurement system is a illuminance meter moving on a sphere surface around the measurement object, as in Figure 6. The illuminance meter is located at the position $(\bar{R},\alpha_s,\beta_s)$ or $(x,y,z)$. With:

$$x = \bar{R}\cdot\sin\alpha_s\cdot\cos\beta_s \qquad y = \bar{R}\cdot\sin\alpha_s\cdot\sin\beta_s \qquad z = \bar{R}\cdot\cos\alpha_s \tag{16}$$

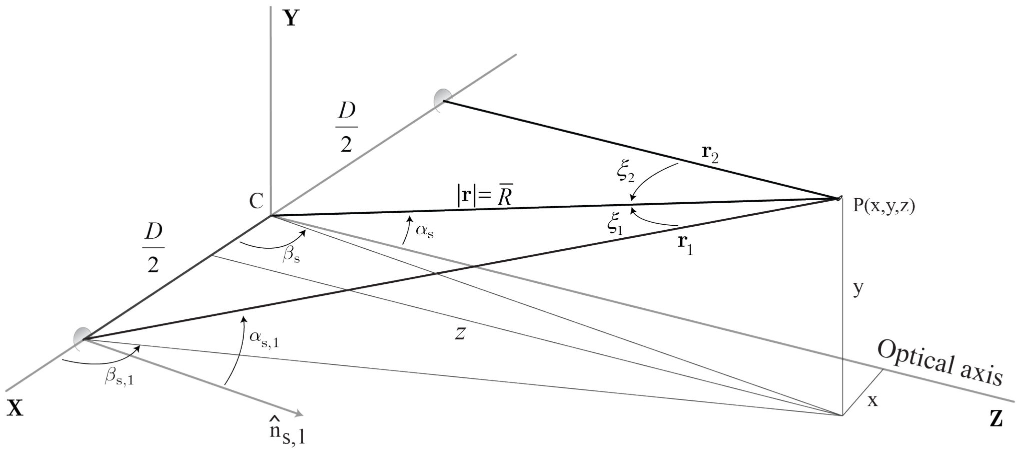


**Figure 6 – The point source approach is illustrated using 2 point sources that are separated by a distance $D$ along the x-axis.**

And for the vectors $\mathbf{r}_1$ and $\mathbf{r}_2$ in a Cartesian coordinate system:

$$\mathbf{r}_1 = \begin{bmatrix} \bar{R} \cdot \sin\alpha_s \cdot \cos\beta_s + \frac{D}{2} \\ \bar{R} \cdot \sin\alpha_s \cdot \sin\beta \\ \bar{R} \cdot \cos\alpha_s \end{bmatrix} \text{ and } \mathbf{r}_2 = \begin{bmatrix} \bar{R} \cdot \sin\alpha_s \cdot \cos\beta - \frac{D}{2} \\ \bar{R} \cdot \sin\alpha_s \cdot \sin\beta \\ \bar{R} \cdot \cos\alpha_s \end{bmatrix} \tag{17}$$

For the absolute values:

$$\begin{aligned} \mathbf{r}_1 &= \sqrt{\left(\bar{R} \cdot \sin\alpha_s \cdot \cos\beta_s + \frac{D}{2}\right)^2 + \left(\bar{R} \cdot \sin\alpha_s \cdot \sin\beta_s\right)^2 + (\bar{R} \cdot \cos\alpha_s)^2} \\ \mathbf{r}_2 &= \sqrt{\left(\bar{R} \cdot \sin\alpha_s \cdot \cos\beta_s - \frac{D}{2}\right)^2 + \left(\bar{R} \cdot \sin\alpha_s \cdot \sin\beta_s\right)^2 + (\bar{R} \cdot \cos\alpha_s)^2} \end{aligned} \tag{18}$$

With the scalar product
$$\begin{aligned} \vec{r}_1 \cdot \vec{e}_z &= r_1 \cdot \cos\alpha_{s1} = \bar{R} \cdot \cos\alpha_s \qquad & \cos\alpha_{s1} &= \bar{R} \cdot \cos\alpha_s / r_1 \\ \vec{r}_2 \cdot \vec{e}_z &= r_1 \cdot \cos\alpha_{s2} = \bar{R} \cdot \cos\alpha_s \qquad & \cos\alpha_{s2} &= \bar{R} \cdot \cos\alpha_s / r_2 \end{aligned}$$

Using the cosine low $D^2/4 = \bar{R}^2 + r_1^2 - 2 \cdot \bar{R} \cdot r_1 \cdot \cos(\varepsilon_1)$ the angles $\varepsilon_1$ and $\varepsilon_2$ can be calculated as:

$$\cos\varepsilon_1 = \left(\bar{R}^2 + r_1^2 - \frac{D^2}{4}\right) / \left(2\bar{R}r_1\right) \text{ and } \cos\varepsilon_2 = \left(\bar{R}^2 + r_2^2 - \frac{D^2}{4}\right) / \left(2 \cdot \bar{R} \cdot r_2\right) \tag{19}$$

The measured illuminance is given as

$$E_{near} = I_1(\alpha_{s1}) / r_1^2 \cdot \cos(\varepsilon_1) + I_2(\alpha_{s2}) / r_2^2 \cdot \cos(\varepsilon_2) \tag{20}$$

Therefore there is a difference between the measured illuminance (and the luminous intensity calculated with this illuminance $I_{app,\,2\,LID}$ and the luminous intensity (the far-field value $I_{FF,\,2\,LID}$) itself.

$$I_{app,\,2\,LID} = \left(\frac{I_1(\alpha_{s,1})}{r_1^2} \cdot \cos(\varepsilon_1) + \frac{I_2(\alpha_{s,2})}{r_2^2} \cdot \cos(\varepsilon_2)\right) \cdot \bar{R}^2 \tag{21}$$

and

$$I_{FF,\,2\,LID} = I_1(\alpha_s) + I_2(\alpha_s) \tag{22}$$

This difference results from the measuring principle of the far field goniophotometer itself.

The angular distribution of the error can be evaluated graphically by inserting Eq. (21) and Eq. (22) into Eq. (5), which is shown for a few measurement distances in Figure 7.

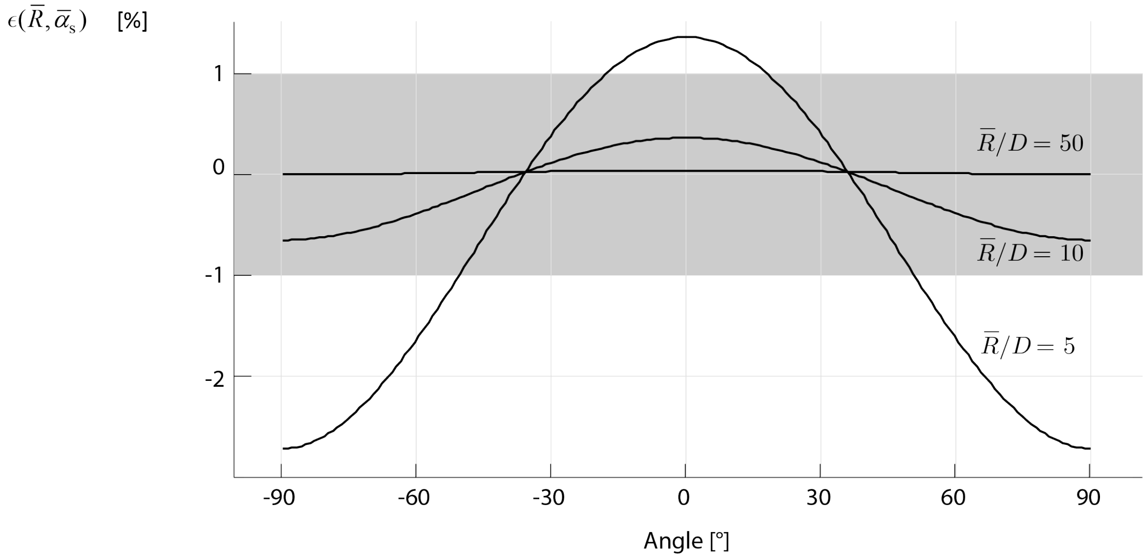


**Figure 7 – Far-field error for a sum of two Lambertian point sources depending on the ratio $\overline{R}/D$ and depending on the angle $\alpha_s$**

## 7 Segmentation approach

An alternative approach, that is not part of this paper, is based on the segmentation of the luminous area. The luminous area is divided into (very) small elements and the same luminous intensity distribution is assigned to each element. This is a common approach in many simulation programs to apply the far field data (luminous intensity distribution) to calculate illuminance values, for example for table surfaces in offices, which are located close to the luminaires. This approach can also be also used to calculate the limiting photometric distance for large light sources. The main advantage here is the possibility to analyse errors for real luminous intensity distributions.

## 8 Rules of thumb

- For Lambertian disk sources, a limiting photometric distance of five times the diameter of the luminaire is sufficient.
- For disk sources with a narrow beam, the limiting photometric distance depends on the beam width and the diameter of the source. Putting $\epsilon = 1\%$, the limiting photometric distance can be calculated using Eq. (10) or estimated using Eq. (12).
- For quasi-1D light luminous stripes, the on-axis limiting photometric distance can be calculated using Eq. (15), while the off-axis behaviour can be derived from the graphical representation in Figure 5.
- For the “worst case scenario” of two point sources, the graphical representation in Figure 7 can be used to estimate the resulting error.

**Table 2: set of rules-of-thumb for determining the error associated with photometric distance.**

| Type of light source | Measurement error for far-field measurements |
|---|---|
| Disk source with diameter *D* Eq. (12) | $\epsilon(\bar{R},0,0)=\frac{n+4}{8}\left[\frac{D}{\bar{R}}\right]^2$ |
| 1D luminous stripe with length *D* (n=0) Eq.(15) | $\epsilon(\bar{R},0,0)=-\frac{1}{6}\left(\frac{D}{\bar{R}}\right)^2$ |
| | Graphical evaluation for off-axis behaviour, using Figure 5 |
| 2 point sources with distance *D* | Graphical evaluation only, using Figure 7 |

## 9 Summary

The luminous intensity distribution is a commonly used model for a light source. In practice however, some errors are introduced due to the use of finite distances to calculate the LID from measured illuminance values. The relation between these errors and the test distance are the topic of this paper.

To study this effect, theoretical derivations are made for a disk-shaped light source, a linear light-strip and the case of two point-sources. Equations are derived for the far-field intensity of these sources, as well as the apparent intensity, which is the intensity that is calculated from a measurement (or calculation) of the illuminance at a finite distance. Also, the limiting photometric distance is defined as the distance where the difference between them is smaller than a predefined threshold of 1%.

The most significant outcome of this work is the analysis of the measurement error not only for the main illumination direction (on-axis) but also for other angles of emission far away from the main illumination direction (off-axis), such as in significant glare areas. The results show how sharply the errors increase with narrower beam angle of a light source. Also, a set of new guidelines are given.

This topic is very relevant at present due to the high variability of LED-based light sources with large gaps between adjacent luminous areas and small size of the light emitting areas. In practice it is difficult to estimate the size of the light source and the influence of the LID to work with the right limiting photometric distance or to estimate the errors that may be encountered measuring particular types of luminaires in a photometric laboratory which has a fixed test distance.

## References

CIE 070-1987, 1987. *The Measurement of Absolute Luminous Intensity Distributions,* Vienna, Austria: CIE.

CIE 121-1996, 1996. *The Photometry and Goniophotometry of Luminaires,* Vienna, Austria: CIE.

CIE S 025/E:2015, 2015. *Test Method for LED lamps, LED luminaires, and LED modules,* s.l.: CIE.

Howell, J. R., Menguc, M. P. & Siegel, R., 2010. *Thermal Radiation Heat Transfer.* 5th Edition ed. s.l.:CRC Press.

ISO/CIE 19476:2014, 2014. *Characterization of the Performance of Illuminance Meters and Luminance Meters. (the former CIE S 023/E:2013) chapter 3.1.9,* s.l.: ISO/CIE.

Jacobs, V., Forment, S., Rombauts, P. & Hanselaer, P., 2014. Near-field and far-field goniophotometry of narrow-beam LED arrays. *Lighting Res. Technology,* Issue 10.1177/1477153514530139.

Moerman, J. J. B. & Holmes, J. G., 1981. The choice of test distance to control errors in the photometry of round projectors focused at a long distance. *Lighting Research and Technology,* Volume Vol. 13, No. 2, pp. 87-95.

Moreno I, S. C.-C. I. R., 2009. Far-field condition for light-emitting diode arrays. *Appl Opt,* 20 Feb., 48(6), p. 1190–7.

Sun C-C, C. W.-T. M. I. H. C.-C. L. Y.-C., 2009. Analysis of the far-field region of LEDs. [Internet]. Available from:. *Opt Express,* 3 Aug., 17(16), p. 13918–27.